Journal of Thermal Analysis and Calorimetry
https://doi.org/10.1007/s10973-023-12862-2

Structural and thermoanalytical characterization of self-healing polymer: the effect of cross-linking density

Tamás Takács[1,2] · Mohamed M. Abdelghafour[1,3] · Dániel Sebők[2] · Ákos Kukovecz[2] · László Janovák[1]

Received: 8 May 2023 / Accepted: 24 December 2023

Abstract

The effect of the gradually formed cross-linked structure on the thermal properties and swelling behaviour of modified poly(vinyl alcohol) was investigated. To this aim, the semi-crystalline polymer was functionalized with aldehyde and amino moieties to produce polymers with dynamic imine cross-links, and, thus, with self-healing or curing ability. With increasing degree of functionalization (0.89–7.12%), denser polymer networks cross-linked by dynamic imine bonds were formed, the samples systematically developed thermoset-like properties compared to the pristine, initially thermoplastic PVA. As a result, the introduction of new moieties into the initial PVA lowered the glass transition (from 65.3 to 35.0 °C) and melting temperatures (from 194 to 161 °C), however, a new peak (T_{crd}) with growing enthalpy values appeared on the DSC curves, which indicates that more and more energy must be supplied in order to break the imine cross-links formed between the introduced aldehyde and amino groups. The significant impact of the degree of functionalization and cross-linking density on the polymer structure was also clearly demonstrated: the crystallinity decreased as the abundance of the introduced moieties increased and the formation of cross-links proceeded. At the same time, the water desorption enthalpies of the samples increased, suggesting a stronger, chemically cross-linked thermoset-like polymer network compared to the thermoplastic poly(vinyl alcohol).

Graphical abstract

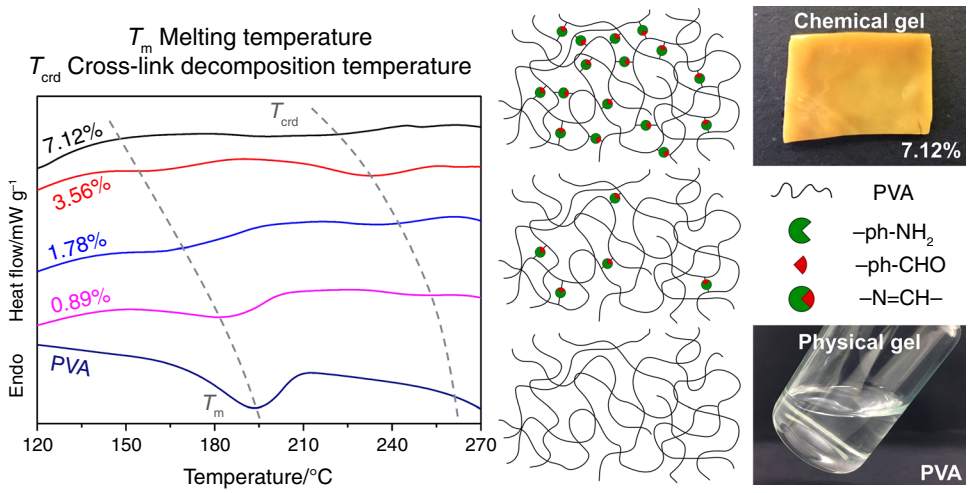

Keywords Poly(vinyl alcohol) · Dynamic Schiff base linkages · Self-curing polymer · Thermoanalytical characterization · Crystallinity

Extended author information available on the last page of the article

Published online: 27 January 2024

Introduction

Polymers can be classified in many ways based on different aspects, such as skeletal structure (linear, branched, cross-linked, ring polymers), repeating units (homo- and copolymers) but most often, they are divided into three main groups depending on their thermal behaviour: thermoplastics, thermosets and elastomers. Thermoplastics represent a significant part of commercial polymers and will be in the focus of the present work.

Thermoplastics are linear or branched polymers that become viscous melts when heated above a specific temperature. Thermoplastics can be either amorphous or (semi-)crystalline. Amorphous polymers don't have crystalline regions, consequently, they cannot be described by the conventional melting temperature (T_m). Instead, the glass transition temperature (T_g) is introduced, above which the „frozen" polymer chains regain their mobility and transition from a glassy state (stiff, hard, brittle polymer) into a rubbery state (soft polymer). In contrast to the amorphous thermoplastics, their (semi-)crystalline counterparts contain both crystalline and amorphous regions that can be characterized by T_m and T_g, respectively [1]. It is also worth mentioning that amorphous polymers exhibit lower thermal stability due to their higher oxygen permeability [2].

Poly(vinyl alcohol) (PVA) is one of today's most widely used water-soluble thermoplastics. It is a linear, semi-crystalline, biodegradable polymer with excellent biocompatibility and film-forming ability [3–8]. It is used in biomedicine (tissue engineering [9, 10], wound dressings [11–13], drug delivery systems [5, 14–16]), in cosmetics (stabilizing agent [17], thickener [18, 19]), in food and many other industries as packaging material [20–23]. The high concentration of hydroxyl groups in PVA offers a great possibility for the functionalization and/or the physical/chemical cross-linking of the polymer to improve its properties. Frequently utilized methods to chemically cross-link PVA: (1) cross-linking with di-/multifunctional compounds (e.g. glutaraldehyde [24], glyoxal [25] under acidic conditions, diisocyanates [26]), (2) functionalization and the subsequent reaction of the introduced groups to form cross-links [27, 28], (3) functionalization and the use of di-/multifunctional compounds to cross-link the introduced side groups [29], (4) cross-linking by irradiation (e.g. electron beam [30], γ-rays [31]).

In order to maximize the performance of cross-linked/functionalized polymers in the desired fields of application, their physicochemical, mechanical and thermal properties must be extensively studied. Knowing the thermal characteristics (e.g. T_g, T_m, thermal stability, etc.) is of the utmost importance since they determine how the polymer can be processed and where it can be utilized.

The thermal properties of PVA are greatly affected by the formation of hydrogen bonds due to the abundance of hydroxyl groups. The polymer shows a large, well-defined endotherm peak around 200 °C which can be attributed to the T_m (230 °C [32], 185 °C [33]) of the polymer. J.S. Park's work describes the effect of chemical cross-linking on T_m of PVA: as the concentration of the glutaraldehyde increased, the reduction of the melting peak intensity and the shift towards lower temperature values were observed. It was discovered by Giménez et al. that the introduction of bulky, rigid pendant groups into the polymer caused an increase in T_m (240–260 °C) [33]. The same trends can be observed in the case of T_g: whereas cross-linking with glutaraldehyde [32] or with different dianhydrides [34] led to lower T_gs compared to the initial T_g (85 °C [32], 82.9 [34], 46 °C [33]) of the pristine PVA, the modification of polymer chains with rigid, bulky moieties resulted in higher T_gs (46–88 °C) [33]. On the other hand, both the cross-linking of PVA with glutaraldehyde and the functionalization with rigid, bulky moieties resulted in improved thermal stability of the polymer [32, 33, 35]. However, it must be pointed out that no universal correlation can be derived with regards to the changes of T_m, T_g values and thermal stability because different factors such as size and structure of molecules used for cross-linking/functionalization, cross-linking density, degree of functionalization, and some properties of the pristine polymer (backbone mobility, crystallinity, degree of hydrolysis, water content, etc.) [32, 36–39] have a combined effect on the thermal properties and therefore always must be studied with respect to the given polymer [26].

In our previous study, the modification of PVA with 4-formylbenzoic acid (4-FBA) and 3,4-diaminobenzoic acid (3,4-DABA) was described [28]. The formation of dynamic Schiff base linkages, which resulted from the interaction of the aldehyde and amino moieties, generated a reversible covalent network with unique autonomous self-healing abilities. However, the introduction of new functionalities into the polymer and the formation of the reversible imine cross-links greatly affect the thermal, mechanical and physicochemical properties, and, thus, the processability of the polymer. The importance of investigating the effects of functionalization on the above-mentioned properties of PVA is described in this manuscript.

Experimental

Materials

For the synthesis of the polymers, PVA (M_w = 46.83 kDa; degree of hydrolysis: 86–89%) was acquired from Nagart Kft., while 4-formylbenzoic acid (4-FBA, 97%), 3,4-diaminobenzoic acid (3,4-DABA, 97%),

N,*N*′-dicyclohexylcarbodiimide (DCC, 99%) and 4-(dimethylamino) pyridine (DMAP, ≥ 99%) were purchased from Sigma-Aldrich. Dimethyl sulfoxide (DMSO, ≥ 99.9%) was obtained from Merck.

Preparation of the polymer films

The procedure for the preparation of modified PVA polymer films was described in great detail in our previous publication [28]: 5.0 g PVA (M_w = 46.83 kDa) was dissolved in 100.0 mL of DMSO without heating. Then, 4-formylbenzoic acid, DCC and catalytic amount (10% molar equivalence to DCC) of DMAP were added to the PVA/DMSO solution, followed by the addition of 3,4-diaminobenzoic acid. The reaction mixture was stirred at 25 °C for 24 h. The urea byproduct of DCC was removed by filtration. The reaction mixture was concentrated by heating, the polymer was obtained by precipitation with acetone and was separated from the liquid phase by centrifugation (5000 rpm, 25 min; Hettich Universal 30F centrifuge). Finally, the acquired polymer was dried at room temperature to constant mass. Next, the dried polymers were dissolved/swollen in distilled water. Subsequently, the polymer solutions (11.25 w/v%) were poured into Petri dishes and dried at 40 °C to constant mass, resulting in free-standing films. For the swollen state (i.e. hydrogel) studies, 50 ± 0.6 mg of the dry polymer samples were equilibrated at room temperature in 125 µL distilled water for one week. Since the films cast of the pristine PVA and all the other modified polymers dissolve in distilled water apart from the one with a nominal degree of functionalization of 7.12%, the samples were swollen in a small amount of water. Based on the added amount of water, the water content of the gels was calculated to be ca. 71 mass%. Next, the values of enthalpy of desorption/vaporization (ΔH_{vap}) were determined by differential scanning calorimetry.

Characterization

The Attenuated Total Reflection Fourier Transform Infrared Spectroscopy (ATR-FTIR) measurements were performed using a BioRad FTS-60A FTIR spectrometer. The spectra were registered between 4000 and 600 cm^{-1} by accumulating 32 scans at a resolution of 4 cm^{-1}.

The X-ray diffractograms of the pristine PVA and the modified polymer films were recorded on a Philips X-ray diffractometer (XRD) with Cu Kα (= 0.1542 nm) as the radiation source at ambient temperature in the 10–60° (2θ) range applying 0.02° (2θ) step size.

The thermal behaviour of the polymer films in dry and swollen states was investigated by using differential scanning calorimetry (DSC). The DSC measurements were carried out by utilizing a Mettler Toledo DSC 822e instrument. For the dry state investigations, the polymer samples were heated in the temperature range of 25–250 °C at a rate of 2.5 °C min^{-1} in a sealed aluminium sample holder with a hole at the top. In the previous publication, an attempt was also made to find the T_gs of the polymer films, however, this was only possible for the pristine PVA, whereas in the case of the modified polymer films, T_gs could not be identified [28]. This issue probably arose from the interfering effect of the evaporation of water remaining in the polymer films after the drying step and the moisture that was absorbed from the air during the storage of the samples. In order to resolve the problem, an additional drying step at 60 °C was included directly before new DSC measurements were carried out. To make sure that the thermal events have enough time to occur, the heating rate was set to 2.5 °C min^{-1}. The swollen samples were studied in the temperature range of 25–200 °C at a heating rate of 5 °C min^{-1} following the same measurement procedure. In the course of the evaluation of DSC curves, values of ΔH_{vap} were calculated from the areas under the peaks and normalized to the water contents (71 mass%) of the swollen hydrogels. Nitrogen was used as the carrier gas at a flow rate of 50 mL min^{-1}. Each experiment was carried out in triplicate and the data were all averaged.

Results and discussion

Structural characterization

In our previous paper, the results of digital microscopy, scanning electron microscopy, X-ray micro-computed tomography and tensile tests were presented in great detail, which demonstrated well the self-healing properties of the functionalized polymers [28]. As clearly shown by the tensile tests, the formation of imine cross-links significantly affected the mechanical properties of the polymers and gave them the capability to self-heal. It could be observed that the neat PVA film exhibited minimal self-healing capacity (which may be attributable to the self-adhesion of PVA, hence the term "Healed" PVA) and the "healed" PVA film had poorer mechanical properties than the virgin sample. In contrast, the functionalized polymer film displayed a high healing efficiency and the healed sample possessed similar mechanical properties to that of the undamaged modified PVA film (Fig. 1a). For this reason, the current work was devoted to the investigation of the effects of imine bond formation on the crystallinity and thermoanalytical properties of the samples.

The formation of imine bonds was studied with FTIR spectroscopy and detailed spectra were shown in our previous publication [28]. In this work, only the spectral region of 1670–1510 cm^{-1} is demonstrated, which confirms the successful functionalization and imine bond formation between

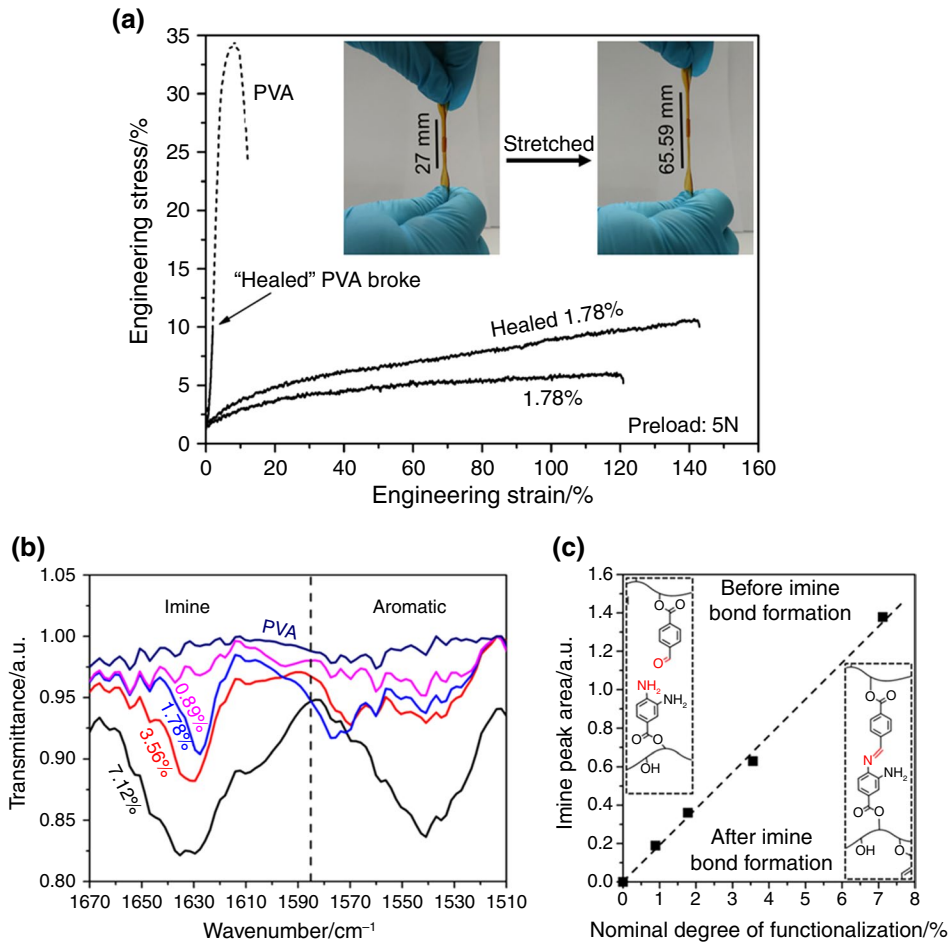

Fig. 1 **a** Stress–strain curves of the neat PVA and a modified polymer film (nominal degree of functionalization: 1.78%) before and after healing at room temperature for 24 h, the inset shows the extensibility of the healed sample; **b** the relevant section of the FTIR spectra of pristine PVA and the modified polymers with different nominal degrees of functionalization; **c** areas of peaks related to the imine bond (1635–1628 cm^{-1}) as a function of the nominal degree of functionalization; The dashed line is a guide to the eye

aldehyde and amino groups (Fig. 1b). With increasing nominal degree of functionalization, a band was observed with gradually increasing intensity with a maximum at 1635–1628 cm^{-1}. This band was attributed to C=N stretching vibration, indicating the formation of imine cross-links in the polymer films [40]. Furthermore, the peak appearing around 1540 cm^{-1} can be assigned to the aromatic C=C bending vibrations suggesting the successful modification of PVA [41]. The imine cross-link density may be assessed quantitatively by determining the areas under the corresponding absorption bands. It was observed that as the extent of modification increased, the area under the C=N band also increased continuously, suggesting a gradual increase in the cross-linking density (Fig. 1c). The degrees of crystallinity of the PVA samples were also estimated via ATR-FTIR spectroscopy, according to the method reported by Peppas [42] and the values varied between 46–9% (see later).

The effect of functionalization on the crystallinity of the PVA films was also investigated by XRD (Fig. 2). For the pristine PVA, the characteristic reflections observed at 2θ ~ 11.2°, 19.4°, 22.7° and 40.5° in the range of 10–60° are in good agreement with the values reported in the literature [43–45]. The peaks at 2θ ~ 11.2° and

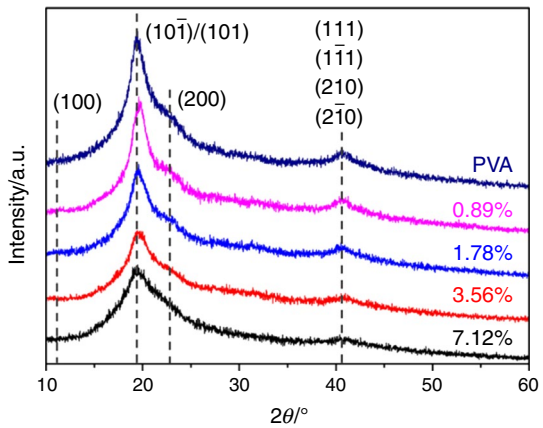

Fig. 2 XRD patterns of the pristine PVA and the modified polymer films with different nominal degrees of functionalization

40.5° correspond to the (100) and a compound of (111), (1 1 1), (210), (2 1 0) crystalline planes, respectively. The main diffraction peak at 2θ ~ 19–20° originates from the overlapping reflections from the (10 1) and (101) planes, whereas its shoulder at 2θ ~ 22.7° can be attributed to

the (200) reflection [43, 44]. As shown in Fig. 2, with increasing nominal degree of functionalization, the diffraction peaks gradually broadened, their intensities systematically diminished, which suggested a decrease in the crystallinity of the samples.

This trend was also corroborated by the determined degree of crystallinity values. In order to estimate the degrees of crystallinity of the samples, the relevant parts of the diffractograms in the range of 10–30° were resolved into crystalline and amorphous components by utilizing a Gaussian curve fitting method, as shown in Fig. 3. The resolved diffraction pattern for the pristine PVA film (Fig. 3a) revealed five characteristic contributions from the (100), (001), (10 $\bar{1}$), (101) and (200) crystalline planes with peak maxima at 2θ ~ 11.2°, 17.8°, 19.4°, 19.7° and 22.7°, respectively, which is in accord with the data reported in the literature [43, 45]. Since the reflection at 2θ ~ 19.4° arises from the main crystalline plane, it is the most suitable candidate to follow the changes in crystallinity of the samples, as the nominal degree of functionalization is varied. The ratio of the area under the crystalline peaks to the sum of the areas under the crystalline and amorphous contributions can give a good estimation of the degrees of crystallinity of the polymer films. The crystallinity of the pristine PVA film was estimated at 37%, whereas with the gradually increasing extent of modification (from 0 to 7.12%), the crystallinity of the samples systematically decreased up to 8%.

To further assess the changes in the crystallinity of the polymer films, the full width at half maximum (FWHM) values of the peaks obtained by deconvolution were determined for every sample and the ratio of the FWHM values of the crystalline peaks to the sum of the FWHM values of all peaks was calculated. The FWHM ratios decreased as the degree of functionalization increased, suggesting an increasing structural disorder of the polymer chains (Fig. 4).

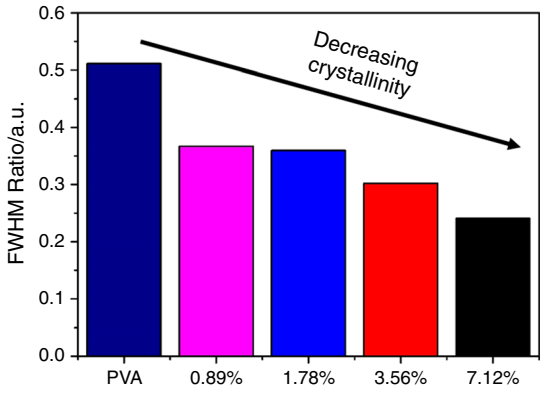

Fig. 4 The ratio of the FWHM values of the crystalline peaks to the sum of the FWHM values of all peaks

Thermal properties

In dry state

The thermal properties of polymer films prepared from the pristine (physically cross-linked) PVA and modified polymers (chemically cross-linked) were partly investigated with DSC and TGA techniques, the results of which were published in a previous publication [28]. DSC measurements carried out in a wider temperature range (Fig. 5a) showed that the extent of functionalization had a significant effect on the thermal properties of the polymer films: the melting peaks (T_m) of polymer films with increasing nominal degree (0.89–7.12%) of functionalization broadened gradually (Fig. 5a) and shifted to lower temperature values (from 194 to 161 °C), whereas in the case of the sample with the highest degree of functionalization (7.12%), the peak corresponding to the melting transition could not be observed (Fig. 6a).

The enthalpy of melting (ΔH_m) values were also determined by the integration of the melting peaks which showed a declining trend as the extent of modification increased

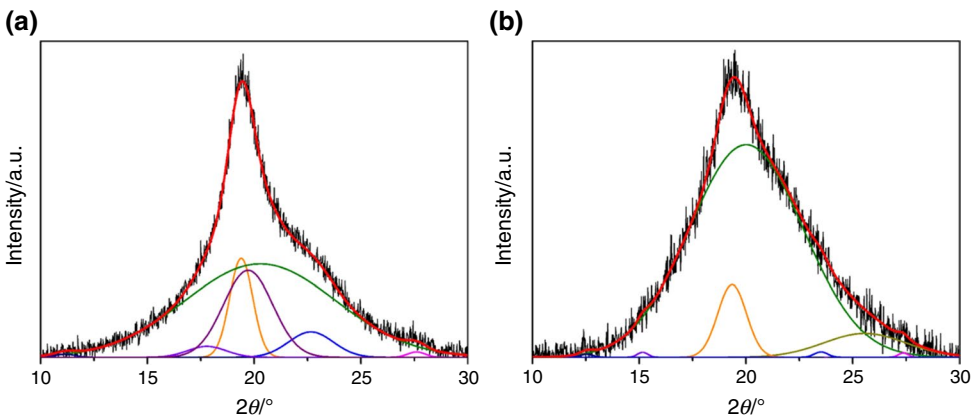

Fig. 3 Deconvoluted XRD patterns of the pristine PVA film (**a**) and the modified polymer film with a nominal degree of functionalization of 7.12% (**b**)

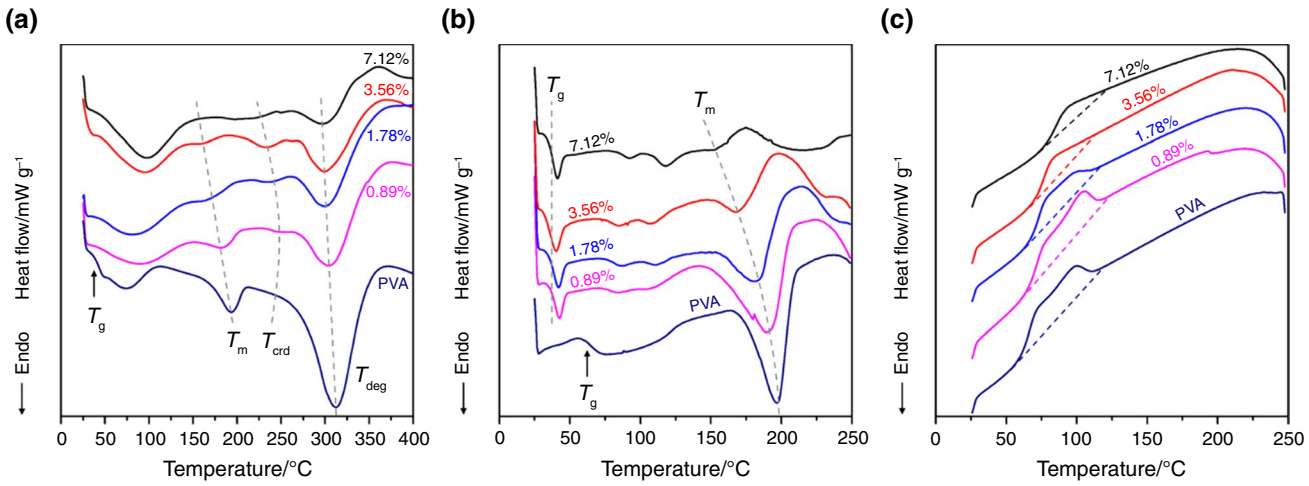

Fig. 5 **a** DSC curves of the pristine PVA and the modified polymers with different nominal degrees of functionalization (temperature range: 25–400 °C, heating rate: 5 °C min^{-1}, N_2 atmosphere); **b** heating and **c** cooling curves of the repeated DSC measurements (temperature range: 25–250 °C, heating rate: 2.5 °C min.$^{-1}$, N_2 atmosphere)

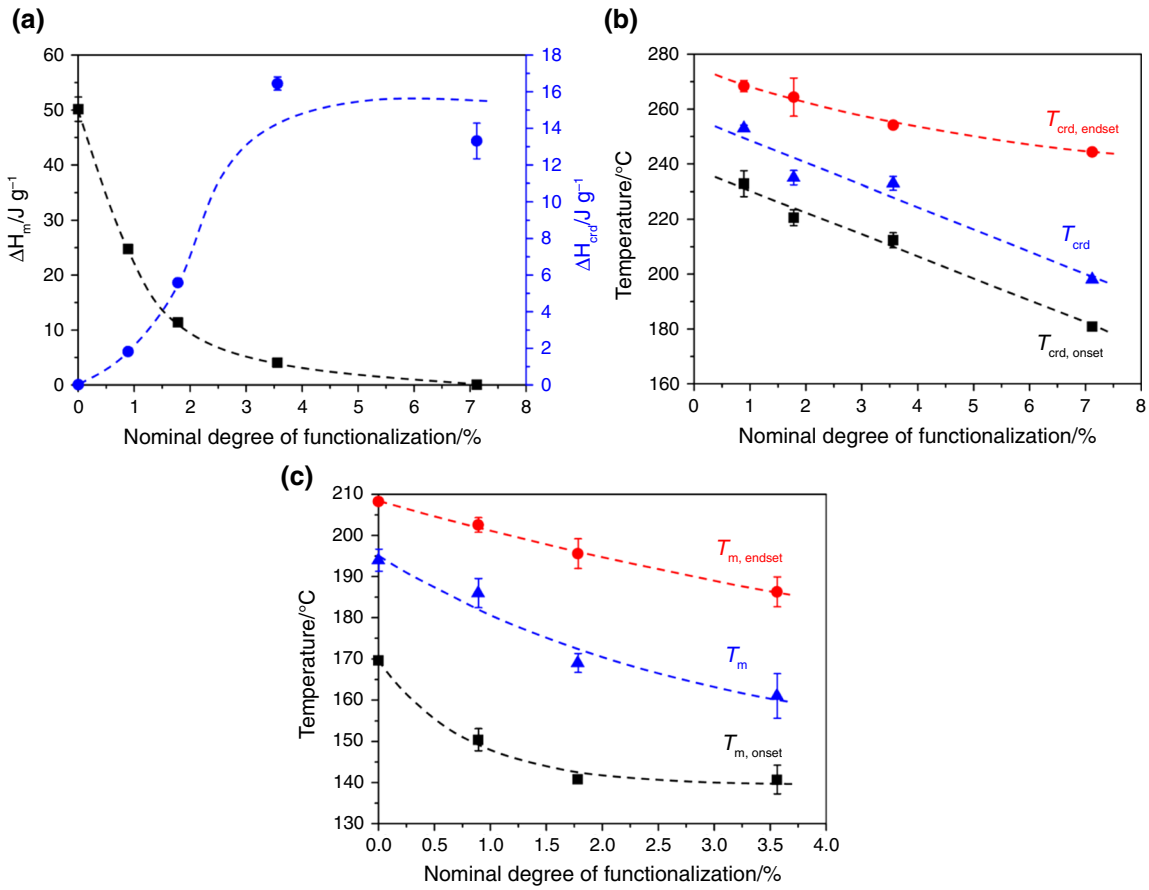

Fig. 6 **a** The enthalpy of melting (ΔH_m) values and the amounts of energy (ΔH_{crd}) that must be supplied to break the cross-links as a function of the nominal degree of functionalization; **b** T_{crd}, $T_{crd,onset}$, $T_{crd,endset}$ and **c** T_m, $T_{m,onset}$, $T_{m,endset}$ values of the pristine PVA and the modified polymers as a function of the nominal degree of functionalization; ihe dashed lines are a guide to the eye

(Fig. 6a and c). Both the changes of melting peaks (broadening, shifting) and the corresponding enthalpies, as also described by J.S. Park et al. [32], suggested the gradual amorphization of the samples. Moreover, with increasing degree of functionalization, new peaks (T_{crd}) with growing enthalpy values appeared (Fig. 5a), which indicates that more and more energy must be supplied in order to break the imine cross-links formed between the introduced aldehyde and amino groups (Fig. 6a and b).

From the DSC curves (Fig. 5a), the degrees of crystallinity of the modified PVA films were determined. ΔH_ms of the samples were divided by the ΔH_m of 100% crystalline PVA (138.6 J g^{-1}, hypothetical value [46]). The crystallinity obtained for the pristine PVA film was 36% which gradually decreased (from 36 to 0%) as the extent of modification increased. In the case of the sample with a nominal degree of functionalization of 7.12%, no ΔH_m could be calculated and therefore the degree of crystallinity was considered to be 0%. The degree of crystallinity values determined this way (36–0%) correspond well with the values obtained from the XRD measurements (37–8%).

Furthermore, it could also be observed that the presence of pendant aldehyde and amino functional groups and the formed reversible covalent network also influenced the T_gs of the polymers (Fig. 5b and c).

By investigating the obtained heating curves (Fig. 5b), the T_gs of the samples could be located (Fig. 7). The pristine PVA possessed the highest T_g (65.3 °C), whereas those of the modified polymer films decreased as the nominal degree of functionalization increased. The introduction of new moieties into the PVA disrupted the polymer's ordered hydrogen-bonded/crystalline regions, which led to the lowering of T_gs (from 65.3 to 35.0 °C) due to the enhanced chain mobility.

As mentioned above, the DSC heating curve of pristine PVA displayed a T_m at 194 °C, whereas the melting peaks of the modified samples shifted to lower temperatures with increasing nominal degree of functionalization (Fig. 5a and b). The DSC cooling curves of the polymer films, shown in Fig. 5c, exhibited characteristic exothermic transitions related to crystallization. In the case of each sample, the crystallization process occurred in a considerably lower temperature range (60–110 °C) compared to the melting transition (194–161 °C). This is because crystallization is a thermodynamic transition governed by kinetics, whereas melting is a purely thermodynamic process. In order for the polymers to crystallize, the macromolecular chains have to arrange themselves into ordered structures, and since it is a sluggish process, it causes crystallization to occur at lower temperatures. Moreover, with the introduction of bulky side groups, the arrangement of polymer chains was further impeded, hindering the crystallization

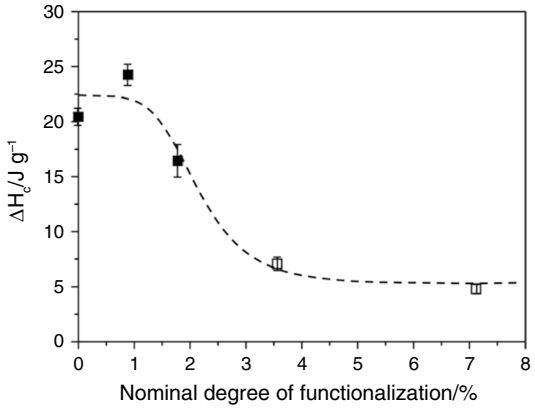

Fig. 8 Enthalpy of crystallization (ΔH_c) values determined by the integration of the part of the DSC cooling curves in the temperature range of 60–110 °C, In the case of samples with degrees of functionalization of 3.56 and 7.12% the indicated ΔH_cs are estimates rather than exact values; the dashed line is a guide to the eye

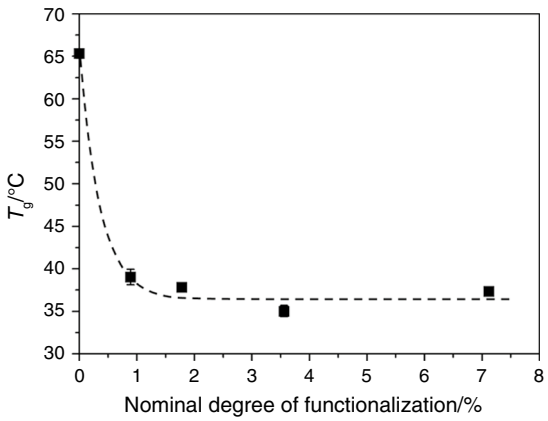

Fig. 7 The change in glass transition temperatures (T_g) with the nominal degree of functionalization; the dashed line is a guide to the eye

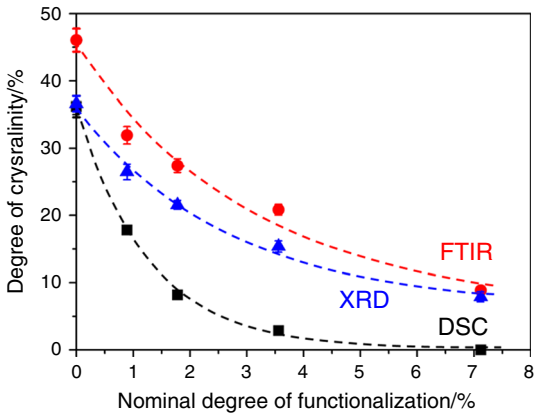

Fig. 9 Estimated degree of crystallinity values based on ATR-FTIR, XRD and DSC methods as a function of the nominal degree of functionalization; the dashed lines are a guide to the eye

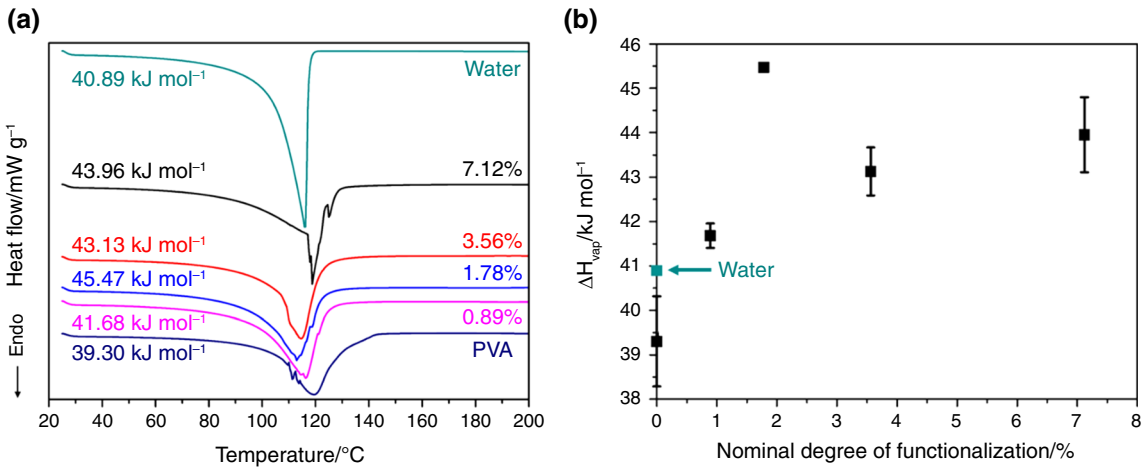

Fig. 10 **a** DSC curves of the swollen pristine PVA and the modified polymer samples with different nominal degrees of functionalization (temperature range: 25–200 °C, heating rate: 5 °C min^{-1}, N_2 atmosphere), The water desorption enthalpy (ΔH_{vap}) values are also represented; **b** dependence of the ΔH_{vap} of the equilibrium-swollen hydrogels on the nominal degree of functionalization

of the samples. In accordance with that, the enthalpies of crystallization (ΔH_c) determined from the cooling curves showed a decreasing trend with increasing extent of modification (Fig. 8). It could also be observed that the crystallization process systematically diminished as the extent of modification increased. For the samples with degrees of functionalization of 3.56 and 7.12%, no distinct exothermic transitions related to crystallization could be detected, so the ΔH_c values were only estimated.

Figure 9 summarizes the estimated degrees of crystallinity of the polymer films determined by ATR-FTIR spectroscopic, XRD and DSC techniques. The trends in crystallinity were found to be in good accord with each other. The differences between the calculated values might have arisen from the application of different analytical techniques.

Thermal properties of swollen hydrogels

In order to determine the amounts of heat required to remove the water content of the swollen hydrogels, i.e. enthalpy of desorption/vaporization (ΔH_{vap}), the thermoanalytical properties of the polymers were also investigated in their swollen states. Figure 10a shows the DSC curves of the swollen polymer films as well as that of the pure distilled water which served as a reference. The ΔH_{vap} values, which are equal to the areas beneath the peaks, are also displayed in the figure. The pristine PVA-based hydrogel had a similar ΔH_{vap} value (39.30 kJ mol^{-1}) to that obtained for pure water (40.89 kJ mol^{-1}), indicating the good mobility of water in the loose structure of the physically cross-linked hydrogel. When the extent of modification, and, thus, the cross-linking density were increased, the water desorption enthalpies of the hydrogels increased (Fig. 10b) and all of the cross-linked samples showed higher (41.68–45.47 kJ mol^{-1}) values than the pristine PVA (39.30 kJ mol^{-1}). The reason for this is that the cross-linked polymers with stronger and more compact gel structures bound water molecules more strongly.

Conclusions

The functionalization of PVA with aldehyde and amino groups yielded polymer films cross-linked by dynamic imine bonds. These reversible covalent bonds endowed the polymers with self-healing ability and altered their thermoanalytical properties, crystalline structure and swelling behaviour. ATR-FTIR spectroscopic investigations (imine peak area) suggested a gradual increase in cross-linking density with increasing degree of functionalization (0.89–7.12%). XRD studies showed the gradual amorphization of the polymer samples as the extent of modification increased. DSC analysis was utilized to locate the T_gs of the dry polymer films. The modified samples possessed lower T_gs (39.0–35.0 °C) than the pristine PVA (65.3 °C) because the introduced functional groups disrupted the hydrogen-bonded regions of the neat polymer. In the temperature range of 234–250 °C, the appearance of new endothermic peaks (T_{crd}) with increasing ΔH_{crd} values (0–16.4 J g^{-1}) was observed. By heating the modified samples in the above-mentioned temperature range, the breaking of cross-links, i.e. the de-cross-linking of the dynamic polymer network occurred. The crystallization behaviour of the dry materials was also influenced by the chemical modification: with the introduction of aldehyde and amino moieties, the arrangement of polymer chains into ordered structures was impeded

and therefore the crystallization process of PVA was hindered. For the samples with degrees of functionalization of 3.56 and 7.12%, no distinct exothermic transitions related to crystallization could be detected, which indicated that the modified polymers became more thermoset-like compared to the pristine, thermoplastic PVA. The swelling properties of the modified polymers were also investigated. The gel structure is significantly affected by the degree of functionalization and binds water with varying strength based on the cross-linking density. The ΔH_{vap} values of the samples were higher (41.68–45.47 kJ mol^{-1}) than that of the pristine PVA (39.30 kJ mol^{-1}), indicating a stronger, cross-linked hydrogel structure. The degree of crystallinity values of the dry, modified PVA films obtained by employing three different techniques varied between 0 and 46% and unanimously showed that the cross-linking density greatly affects the formation of crystalline structures of the samples, thus influencing the thermal characteristics (location of T_g, T_m, T_c) and swelling behaviour of the materials.

Acknowledgements The authors are very thankful for the financial support from the Hungarian Scientific Research Fund (OTKA) K 132446. This paper was also supported by the UNKP-23-5 New National Excellence Program of the Ministry for Innovation and Technology from the National Research, Development and Innovation Fund as well as by the János Bolyai Research Scholarship of the Hungarian Academy of Sciences (L.J.). Project no. TKP2021-NVA-19 has been implemented with the support provided by the Ministry of Innovation and Technology of Hungary from the National Research, Development and Innovation Fund, financed under the TKP2021-NVA funding scheme. M.M.A. is funded by a scholarship under the joint executive program of the Arab Republic of Egypt and Hungary. M.M.A. acknowledges Stipendium Hungaricum for his PhD scholarship. The authors are also very thankful for the financial support from the Interdisciplinary Research Development and Innovation, Center of Excellence, University of Szeged. The publication was funded by The University of Szeged Open Access Fund (FundRef, Grant No. 5480).

Author's contribution TT: investigation, validation, writing—original draft. MMA: investigation, validation. DS: investigation, writing—review and editing. ÁK: supervision, conceptualization, writing—original draft. LJ: supervision, conceptualization, methodology, writing—original draft.

Declarations

Conflict of interests The authors declare that they have no known competing financial interests or personal relationships that could have appeared to influence the work reported in this paper.

References

1. Young RJ, Lovell PA. Introduction to polymers. 3rd ed. Boca Raton: CRC Press; 2011.
2. Tomić NZ. Thermal studies of compatibilized polymer blends. In: Ajitha AR, Thomas S, editors. Compatibilization of polymer blends. Elsevier; 2020. pp. 490–1. https://doi.org/10.1016/C2017-0-03891-0
3. Jiang Z, Diggle B, Tan ML, Viktorova J, Bennett CW, Connal LA. Extrusion 3D printing of polymeric materials with advanced properties. Adv Sci. 2020;7:1–32. https://doi.org/10.1002/advs.202001379.
4. Ben Halima N. Poly(vinyl alcohol): review of its promising applications and insights into biodegradation. RSC Adv. 2016;6:39823–32. https://doi.org/10.1039/c6ra05742j.
5. Rivera-Hernández G, Antunes-Ricardo M, Martínez-Morales P, Sánchez ML. Polyvinyl alcohol based-drug delivery systems for cancer treatment. Int J Pharm. 2021. https://doi.org/10.1016/j.ijpharm.2021.120478.
6. Wu F, Misra M, Mohanty AK. Challenges and new opportunities on barrier performance of biodegradable polymers for sustainable packaging. Prog Polym Sci. 2021;117: 101395. https://doi.org/10.1016/j.progpolymsci.2021.101395.
7. Gong X, Zhang L, He S, Jiang S, Wang W, Wu Y. Rewritable superhydrophobic coatings fabricated using water-soluble polyvinyl alcohol. Mater Des. 2020;196: 109112. https://doi.org/10.1016/j.matdes.2020.109112.
8. Yang X, Sha D, Sun L, Chen L, Xu J, Shi K, Yu C, Wang B, Ji X. Charged group-modified poly(vinyl alcohol) hydrogels: Preparation and antibacterial property. React Funct Polym. 2020. https://doi.org/10.1016/j.reactfunctpolym.2020.104635.
9. Dattola E, Parrotta EI, Scalise S, Perozziello G, Limongi T, Candeloro P, Coluccio ML, Maletta C, Bruno L, De Angelis MT, Santamaria G, Mollace V, Lamanna E, Di Fabrizio E, Cuda G. Development of 3D PVA scaffolds for cardiac tissue engineering and cell screening applications. RSC Adv. 2019;9:4246–57. https://doi.org/10.1039/C8RA08187E.
10. Teixeira MA, Amorim MTP, Felgueiras HP. Poly(vinyl alcohol)-based nanofibrous electrospun scaffolds for tissue engineering applications. Polymers (Basel). 2020. https://doi.org/10.3390/polym12010007.
11. Kamoun EA, Kenawy ERS, Chen X. A review on polymeric hydrogel membranes for wound dressing applications: PVA-based hydrogel dressings. J Adv Res. 2017;8:217–33. https://doi.org/10.1016/j.jare.2017.01.005.
12. Adeli H, Khorasani MT, Parvazinia M. Wound dressing based on electrospun PVA/chitosan/starch nanofibrous mats: fabrication, antibacterial and cytocompatibility evaluation and in vitro healing assay. Int J Biol Macromol. 2019;122:238–54. https://doi.org/10.1016/j.ijbiomac.2018.10.115.
13. Sadeghi-Aghbash M, Rahimnejad M, Adeli H, Feizi F. Fabrication and development of PVA/Alginate nanofibrous mats containing *Arnebia euchroma* extract as a burn wound dressing. React Funct Polym. 2022;181: 105440. https://doi.org/10.1016/j.reactfunctpolym.2022.105440.
14. Chen W, Hou Y, Tu Z, Gao L, Haag R. pH-degradable PVA-based nanogels via photo-crosslinking of thermo-preinduced nanoaggregates for controlled drug delivery. J Control Release. 2017;259:160–7. https://doi.org/10.1016/j.jconrel.2016.10.032.

15. El-Naggar AWM, Senna MM, Mostafa TA, Helal RH. Radiation synthesis and drug delivery properties of interpenetrating networks (IPNs) based on poly(vinyl alcohol)/ methylcellulose blend hydrogels. Int J Biol Macromol. 2017;102:1045–51. https://doi.org/10.1016/j.ijbiomac.2017.04.084.
16. Tampau A, González-Martínez C, Chiralt A. Polyvinyl alcohol-based materials encapsulating carvacrol obtained by solvent casting and electrospinning. React Funct Polym. 2020;153: 104603. https://doi.org/10.1016/j.reactfunctpolym.2020.104603.
17. Thananukul K, Kaewsaneha C, Sreearunothai P, Petchsuk A, Buchatip S, Supmak W, Nim B, Okubo M, Opaprakasit P. Biocompatible degradable hollow nanoparticles from curable copolymers of polylactic acid for UV-shielding cosmetics. ACS Appl Nano Mater. 2022;5:4473–83. https://doi.org/10.1021/acsanm.2c00606.
18. Pal N, Agarwal M, Gupta R. Green synthesis of guar gum/Ag nanoparticles and their role in peel-off gel for enhanced antibacterial efficiency and optimization using RSM. Int J Biol Macromol. 2022;221:665–78. https://doi.org/10.1016/j.ijbiomac.2022.09.036.
19. Ahmed TA, El-Say KM, Ahmed OAA, Zidan AS. Sterile dosage forms loaded nanosystems for parenteral, nasal, pulmonary and ocular administration. In: Grumezescu Am, editor. Nanoscale fabrication, optimization, scale-up and biological aspects of pharmaceutical nanotechnology. Norwich: William Andrew Publishing; 2018. p. 379. https://doi.org/10.1016/B978-0-12-813629-4.00009-7.
20. Tripathi S, Mehrotra GK, Dutta PK. Physicochemical and bioactivity of cross-linked chitosan-PVA film for food packaging applications. Int J Biol Macromol. 2009;45:372–6. https://doi.org/10.1016/j.ijbiomac.2009.07.006.
21. Liu Y, Wang S, Lan W. Fabrication of antibacterial chitosan-PVA blended film using electrospray technique for food packaging applications. Int J Biol Macromol. 2018;107:848–54. https://doi.org/10.1016/j.ijbiomac.2017.09.044.
22. Yang W, Owczarek JS, Fortunati E, Kozanecki M, Mazzaglia A, Balestra GM, Kenny JM, Torre L, Puglia D. Antioxidant and antibacterial lignin nanoparticles in polyvinyl alcohol/chitosan films for active packaging. Ind Crops Prod. 2016;94:800–11. https://doi.org/10.1016/j.indcrop.2016.09.061.
23. Monteiro VAC, da Silva KT, da Silva LRR, Mattos ALA, de Freitas RM, Mazzetto SE, Lomonaco D, Avelino F. Selective acid precipitation of Kraft lignin: a tool for tailored biobased additives for enhancing PVA films properties for packaging applications. React Funct Polym. 2021. https://doi.org/10.1016/j.reactfunctpolym.2021.104980.
24. Ahmad AL, Yusuf NM, Ooi BS. Preparation and modification of poly (vinyl) alcohol membrane: effect of crosslinking time towards its morphology. Desalination. 2012;287:35–40. https://doi.org/10.1016/j.desal.2011.12.003.
25. Zhang Y, Zhu PC, Edgren D. Crosslinking reaction of poly(vinyl alcohol) with glyoxal. J Polym Res. 2010;17:725–30. https://doi.org/10.1007/s10965-009-9362-z.
26. Benavente R, Mijangos C, Perena JM, Krumova M, López D. Effect of crosslinking on the mechanical and thermal properties of poly (vinyl alcohol). Polymer (Guildf). 2000;41:9265–72.
27. Almutairi FM, Monier M, Alatawi RAS, Alhawiti AS, Al-Rasheed HH, Almutairi TM, Elsayed NH. Synthesis of photo-crosslinkable hydrogel membranes for entrapment of lactase enzyme. React Funct Polym. 2022;172: 105159. https://doi.org/10.1016/j.reactfunctpolym.2022.105159.
28. Takács T, Abdelghafour MM, Lamch Ł, Szenti I, Sebők D, Janovák L, Kukovecz Á. Facile modification of hydroxyl group containing macromolecules provides autonomously self-healing polymers through the formation of dynamic Schiff base linkages. Eur Polym J. 2022. https://doi.org/10.1016/j.eurpolymj.2022.111086.
29. Han X, Wang J, Wang L. Preparation of anion exchange membranes based on pyridine functionalized poly(vinyl alcohol) crosslinked by 1,4-dichlorobutane. J Appl Polym Sci. 2019;136:1–9. https://doi.org/10.1002/app.47395.
30. Peppas NA, Merrill EW. Crosslinked poly(vinyl alcohol) hydrogels as swollen elastic networks. J Appl Polym Sci. 1977;21:1763–70. https://doi.org/10.1002/app.1977.070210704.
31. Fan L, Yang H, Yang J, Peng M, Hu J. Preparation and characterization of chitosan/gelatin/PVA hydrogel for wound dressings. Carbohydr Polym. 2016;146:427–34. https://doi.org/10.1016/j.carbpol.2016.03.002.
32. Park JS, Park JW, Ruckenstein E. On the viscoelastic properties of poly(vinyl alcohol) and chemically crosslinked poly(vinyl alcohol). J Appl Polym Sci. 2001;82:1816–23. https://doi.org/10.1002/app.2023.
33. Giménez V, Mantecón A, Cádiz V. Modification of poly(vinyl alcohol) with acid chlorides and crosslinking with difunctional hardeners. J Polym Sci Part A Polym Chem. 1996;34:925–34. https://doi.org/10.1002/(SICI)1099-0518(19960430)34:6%3c925::AID-POLA1%3e3.0.CO;2-H.
34. Xu S, Shen L, Li C, Wang Y. Properties and pervaporation performance of poly(vinyl alcohol) membranes crosslinked with various dianhydrides. J Appl Polym Sci. 2018;135:15–9. https://doi.org/10.1002/app.46159.
35. Figueiredo KCS, Alves TLM, Borges CP. Poly(vinyl alcohol) films crosslinked by glutaraldehyde under mild conditions. J Appl Polym Sci. 2009;111:3074–80. https://doi.org/10.1002/app.29263.
36. Li L, Xu X, Liu L, Song P, Cao Q, Xu Z, Fang Z, Wang H. Water governs the mechanical properties of poly(vinyl alcohol). Polymer (Guildf). 2021;213: 123330. https://doi.org/10.1016/j.polymer.2020.123330.
37. Rostagno M, Shen S, Ghiviriga I, Miller SA. Sustainable polyvinyl acetals from bioaromatic aldehydes. Polym Chem. 2017;8:5049–59. https://doi.org/10.1039/c7py00205j.
38. Fong RJ, Robertson A, Mallon PE, Thompson RL. The impact of plasticizer and degree of hydrolysis on free volume of poly(vinyl alcohol) films. Polymers (Basel). 2018;10:1–15. https://doi.org/10.3390/POLYM10091036.
39. Xue R, Xin X, Wang L, Shen J, Ji F, Li W, Jia C, Xu G. A systematic study of the effect of molecular weights of polyvinyl alcohol on polyvinyl alcohol–graphene oxide composite hydrogels. Phys Chem Chem Phys. 2015;17:5431–40. https://doi.org/10.1039/c4cp05766j.
40. Li K, Wang J, Li P, Fan Y. Ternary hydrogels with tunable mechanical and self-healing properties based on the synergistic effects of multiple dynamic bonds. J Mater Chem B. 2020;8:4660–71. https://doi.org/10.1039/c9tb02885d.
41. Larkin P. IR and Raman spectra-structure correlations: characteristic group frequencies. In: Elsevier Science Bv editor. Infrared and Raman spectroscopy. Elsevier; 2011. p. 88. https://doi.org/10.1016/B978-0-12-386984-5.10006-0
42. Peppas N. Infrared spectroscopy of semicrystalline poly(vinyl alcohol) networks. Die Makromol Chem. 1977;178:595–601. https://doi.org/10.1002/macp.1977.021780228.
43. Assender HE, Windle AH. Crystallinity in poly(vinyl alcohol). 1. An X-ray diffraction study of atactic PVOH. Polymer (Guildf). 1998;39:4295–302. https://doi.org/10.1016/S0032-3861(97)10296-8.
44. Guimarães Junior M, Teixeira FG, Tonoli GHD. Effect of the nano-fibrillation of bamboo pulp on the thermal, structural, mechanical and physical properties of nanocomposites based on starch/poly(vinyl alcohol) blend. Cellulose. 2018;25:1823–49. https://doi.org/10.1007/s10570-018-1691-9.
45. Liu P, Chen W, Liu C, Tian M, Liu P. A novel poly (vinyl alcohol)/poly (ethylene glycol) scaffold for tissue engineering with a unique bimodal open-celled structure fabricated using

supercritical fluid foaming. Sci Rep. 2019;9:1–12. https://doi.org/10.1038/s41598-019-46061-7.
46. Peppas NA, Hansen PJ. Crystallization kinetics of poly(vinyl alcohol). J Appl Polym Sci. 1982;27:4787–97. https://doi.org/10.1002/app.1982.070271223.

Authors and Affiliations

Tamás Takács[1,2] · Mohamed M. Abdelghafour[1,3] · Dániel Sebők[2] · Ákos Kukovecz[2] · László Janovák[1]

✉ Ákos Kukovecz
kakos@chem.u-szeged.hu

✉ László Janovák
janovakl@chem.u-szeged.hu

[1] Department of Physical Chemistry and Materials Science, University of Szeged, Rerrich Béla Tér 1, 6720 Szeged, Hungary

[2] Department of Applied and Environmental Chemistry, University of Szeged, Rerrich Béla Tér 1, 6720 Szeged, Hungary

[3] Department of Chemistry, Faculty of Science, Zagazig University, Zagazig 44519, Egypt